Materials Research. 2023; 26(suppl. 1): e20220549
DOI: https://doi.org/10.1590/1980-5373-MR-2022-0549

Synthesis and Characterization of Polypyrrole/Fe_3O_4 Nanocomposites: A Promising Material Against Carbon Steel Corrosion

Maurício F. de Aguiar[a]***, Raissa A. Borges***[a]***, Mônica F.B. Rocha***[a]***, Nadège Bouchonneau***[a]***,***
Celso P. de Melo[b]***, Helinando P. de Oliveira***[c]***, Kleber G.B. Alves***[a*]

[a]*Universidade Federal de Pernambuco, Departamento de Engenharia Mecânica, 50670-901, Recife, PE, Brasil.*
[b]*Universidade Federal de Pernambuco, Departamento de Física, 50670-901, Recife, PE, Brasil.*
[c]*Universidade Federal do Vale do São Francisco, Instituto de Pesquisa em Ciência dos Materiais, 48902-300, Juazeiro, BA, Brasil.*

Received: December 14, 2022; Revised: March 20, 2023; Accepted: May 03, 2023

The use of conducting polymers as coating layers for the protection of surfaces against corrosion represents an important topic for investigation, as reported in the literature. In this work, polypyrrole/Fe_3O_4 nanoparticles (Fe_3O_4_NPs/PPy) hybrid nanocomposites (HN) were incorporated as anticorrosive additives in an epoxy paint to protect SAE 1010 carbon steel from corrosion. The HN particles were obtained by chemical polymerization of pyrrole in an aqueous solution in the presence of Fe_3O_4_NPs and were characterized by infrared absorption spectrophotometry, dynamic light scattering (DLS), X-ray diffraction (XRD), transmission electron microscopy (TEM). The electrochemical impedance spectroscopy (EIS) was used in the analysis of the electrochemical response of the coated surface with and without HN. DLS data showed that the Fe_3O_4_NPs and Fe_3O_4_NPs/PPy obtained in solution present average diameters of (19.7 ± 9.6) nm and (63.5 ± 27.7) nm, respectively. TEM images showed Fe_3O_4_NPs with smaller sizes (10 nm - 30 nm), and that the HN had diameters smaller than 100 nm, consisting of Fe_3O_4 cores coated with polypyrrole. EIS measurements have shown that the addition of HN to the epoxy paint could improve the efficiency of the anticorrosive coating when compared to the original epoxy paint prepared without any corrosion inhibitor.

Keywords: *Conducting polymers, nanocomposites, iron oxide, polypyrrole, corrosion.*

1. Introduction

Organic coatings are widely used to protect metal structures from corrosive environments as they can be easily applied at a reasonable cost[1]. In addition, due to its excellent adhesion, good mechanical properties and chemical resistance in various aggressive environments, such as under conditions of high humidity and wet surfaces[2], epoxy resins have been used in a wide variety of polymeric coatings to protect surfaces against corrosion. Most of the primer coatings contain iron oxide as one of their additives[1].

The use of conductive polymers in corrosion protection was reported in 1985, by DeBerry[3] and in 1987, by MacDiarmid and Ahmad[4]. Many studies involving conductive polymers (CP), such as polyaniline, polypyrrole, and polythiophene, have been performed and reported in the literature[5-7], with of aim of investigating the efficiency of conductive polymer coatings in corrosion protection of steels. In this context, polypyrrole (PPy) and polyaniline (PANI), and other CP can also be mixed with non-conductive paints for corrosion control or used as primer coatings[8-11].

The conductive polymer coating acts as an oxidant for the metal substrates, and a stable oxide passivation film is formed. The CP coatings have been investigated and applied in various technological applications due to their peculiar properties, such as good environmental stability, processability, high conductivity, and low cost[10,12].

Several studies also investigated the use of conducting polymer-based nanocomposites for corrosion protection in metal coatings[13-16]. By adding metal, metal oxides, graphene, or graphene oxide in conducting polymers, several works developed hybrid and nanohybrid conducting polymers. Reported results confirmed that these new materials can improve the performance of devices applied in several fields, such as sensors, electronic devices, biomedical applications, or anti-corrosion coatings[15].

On the other hand, magnetite (Fe_3O_4) has found a wide range of applications in several areas, as a result of its good catalytic, electrical, electronic and optical properties[17-19]. In a previous study, PPy/Fe_3O_4 composites were electrochemically synthesized on iron to provide corrosion protection by maintaining the substrate in a passive state[20]. Fe_3O_4 has been pointed out as an interesting support to be used in anti-corrosive coatings due to the characteristic low-cost, which makes this system as a promising support for further studies in corrosion protection.

Herein, it is reported the synthesis, characterization and electrochemical evaluation of Fe_3O_4_NPs and Fe_3O_4_NPs/PPy

---

*e-mail: kleber.gbalves@ufpe.br

nanocomposites by emulsion polymerization. The materials were characterized by the use of several techniques, such as dynamic light scattering (DLS), infrared spectroscopy (FT-IR), X-ray diffraction (XRD) and transmission electron microscopy (TEM). Epoxy coating was used as a binder for the nanoparticles and nanocomposites incorporation as a part of a strategy to confer uniform coatings. Then, it was explored electrochemical impedance spectroscopy (EIS) to study the effect of Fe_3O_4_NPs and Fe_3O_4_NPs/PPy on the corrosion inhibition capability of the epoxy coatings in 3% saline solution at room temperature. To the best of our knowledge, no previous work about the use of Fe_3O_4_NPs/PPy nanocomposites as anticorrosive additives of epoxy paints has been published in the literature. In addition, the novelty of this paper refers to the complete electrical characterization of the kinetics of the corrosive process in negative control coatings and the use of nanocomposite as a coating layer.

2. Experimental

2.1. Materials

Pyrrole monomer (C_4H_5N - Sigma-Aldrich, USA) was previously distilled under a vacuum and subsequently stored in a dark refrigerated environment. All chemical reagents, such as ferrous sulfate heptahydrate ($FeSO_4.7H_2O$ - Reagen, Brazil), ferric chloride hexahydrate ($FeCl_3.6H_2O$ - Synth, Brazil), ammonium hydroxide (NH_4OH - Quimex, Brazil), and sodium dodecyl sulfate ($C_{12}H_{25}NaO_4S$ - Sigma-Aldrich, USA), were of analytical grade and we have used them without purification.

2.2. Preparation of Fe_3O_4_NPs

The Fe_3O_4_NPs were obtained by chemical co-precipitation method[21], as follows: two aqueous solutions were prepared, each one with 25 mL, with the first containing $FeSO_4.7H_2O$ (1.0 M) and the second $FeCl_3.6H_2O$ (1.5 M). Subsequently, these solutions were mixed and added to an aqueous solution of NH_4OH (50%, 50 mL). The resulting solution was kept under stirring for 2 hours and then filtered on a paper filter to collect the suspended material, which was abundantly washed with deionized water, dried in a vacuum oven (60 °C) for 48 hours, and then stored in a desiccator.

2.3. Preparation of Fe_3O_4_NPs/PPy composites

The Fe_3O_4_NPs/PPy composites were prepared by chemical *in situ* polymerization of pyrrole in an aqueous solution containing Fe_3O_4_NPs and sodium dodecyl sulfate (SDS)[21]. The polymerization was conducted in a round bottom 100 mL flask. For this, it was prepared An aqueous solution (20 mL) containing Fe_3O_4 (10 mM) with the surfactant (SDS, 10 mM). The mixture was stirred vigorously for 20 minutes and then the monomer pyrrole (250 µL) was added, with the stirring maintained for one additional hour. Polymerization was initiated as we slowly added 400 µL of a concentrated solution of $FeCl_3$ (1M) to the volumetric flask. The solution was kept under vigorous stirring for 24 hours for ensuring complete polymerization. A stable, colloidal black-colored Fe_3O_4_NPs/PPy composite was formed. To obtain a powder composite material, aliquots of methanol were added in excess to the colloidal dispersion, which was then centrifuged and dried in a vacuum at 60 °C for 24 hours.

2.4. Sample Characterization

The particle size measurement was performed by Dynamic Light Scattering (DLS) using a ZS90 Zetasizer Nano equipment (Malvern Instruments, UK), with a laser wavelength of 633 nm, under a scattering angle of 90°, and 25 °C. The results were obtained by taking into account the average of three measurements performed on each sample. To analyze the morphology of the samples, a Tecnai G2 Spirit (FEI Company, USA) Transmission Electron Microscope (TEM) with 100 kV was used. The samples were deposited in Copper-coated 400 mesh carbon grids. The analysis of vibrational spectroscopy in the infrared region was performed with basis on the use of potassium bromide (KBr) pastilles on an FTLA ABB model 2000 FTIR spectrometer (Bomem, Canada) operating in the region of 2000-400 cm^{-1}, with a 4 cm^{-1} resolution and taking 200 accumulations for each spectrum. The crystal structure of the powder was analyzed in a D5000 diffractometer (Siemens AG, Germany) using Cu Kα radiation ($\lambda = 1.54$ Å). The scan rate used was 0.02^{o}/second in 2θ.

2.5. Preparation of Fe_3O_4_NPs/PPy incorporated into epoxy coating

SAE 1010 carbon steel specimens of size 50 mm x 50 mm x 3 mm were sandblasted (Sa 2.5) and then coated with the developed paint. For the effect of comparison, a commercial epoxy-based paint was used and tested with and without the addition of 0.2% w/w Fe_3O_4_NPs/PPy composites. The coatings were applied over the sand-blasted steel surfaces by immersion and evaluated after 10 days of curing at room temperature.

2.6. Evaluation of corrosion-resistant properties of the coating by EIS studies

Electrochemical Impedance Spectroscopy (EIS) studies were performed using a PGSTAT 302N system (Autolab, Netherlands), at room temperature (24° C). Experimental data were acquired and processed by Nova 1.7 software. The impedance measurements were carried out over a frequency range of 6 kHz to 40 mHz using a 10 mV amplitude of sinusoidal voltage as a perturbing signal. The corrosion cell was equipped with platinum gauze as the counter electrode and Ag/AgCl saturated KCl as a reference electrode. The coated SAE 1010 carbon steel plate was the working electrode. The coating layer thickness was (147 ± 31) µm and the whole tested area of the working electrode was 10.2 cm^2. The coated samples were immersed in 3 wt% NaCl solution at room temperature for 0 to 20 h. This concentration of the solution was chosen as a standard value reported in several previous works[22-26].

3. Results and Discussion

The particle size distribution by DLS is shown in Figure 1. The results indicate that for Fe_3O_4_NPs the average particle diameter obtained was (19.7 ± 9.6) nm (Figure 1a) with a

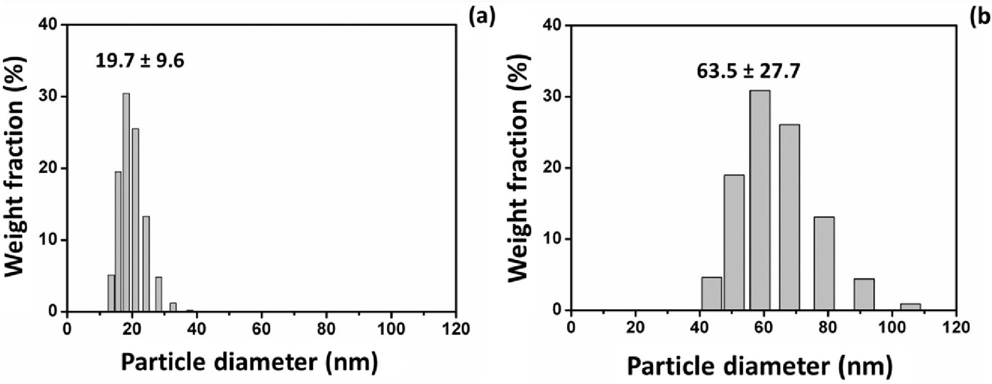

Figure 1. Size distribution of colloidal suspension particles: (a) Fe_3O_4_NPs and (b) Fe_3O_4_NPs/PPy characterized by DLS.

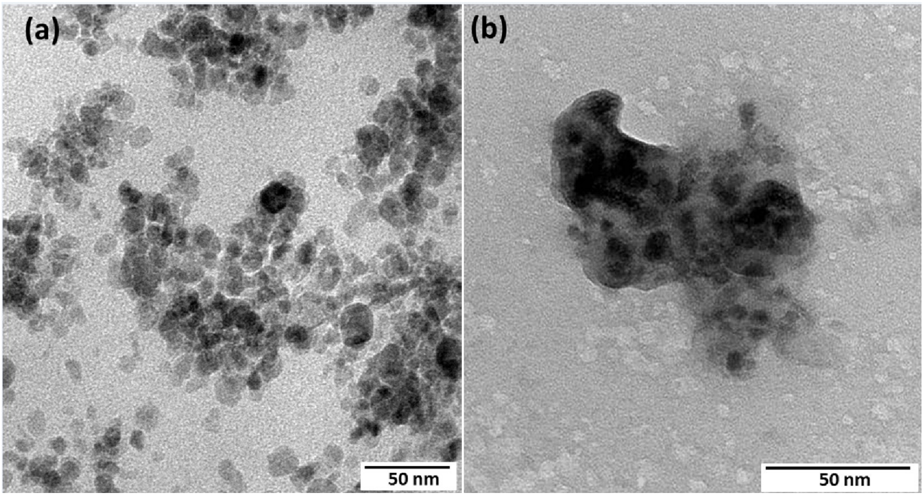

Figure 2. Images obtained by TEM of: (a) Fe_3O_4_NPs and (b) Fe_3O_4_NPs/PPy.

narrow distribution. An average diameter of (63.5 ± 27.7) nm (Figure 1b) was observed for Fe_3O_4_NPs/PPy nanocomposites.

Figure 2 shows the morphology of the Fe_3O_4_NPs and Fe_3O_4_NPs/PPy nanocomposites obtained by TEM. Fe_3O_4_NPs samples were obtained with an average diameter between 10 - 30 nm (see Figure 2a), while the diameter of the Fe_3O_4_NPs/PPy nanocomposite, which is composed of Fe_3O_4_NPs cores coated with polypyrrole, was smaller than 100 nm (Figure 2b).

Patterns of X-ray diffraction (XRD) analysis obtained for the Fe_3O_4_NPs and the Fe_3O_4_NPs/PPy composite are shown in Figure 3. The main diffraction peaks of Fe_3O_4_NPs, which are located at $2\theta = 18.4^o$; 30.2^o; 35.6^o; 43.1^o; 53.6^o, 57.3^o and 62.85^o and correspond to Bragg reflections (111), (220), (311), (400), (422), (511) and (440), respectively, allowed us to identify a cubic structure spinel type for the magnetite phase[27]. These peaks are in agreement with the JCPDS (Joint Committee on Powder Diffraction Standards) 19-0629 data for magnetite according to reported literature[28]. By analyzing the results obtained for the Fe_3O_4_NPs/PPy composite, we observed a decrease in the Fe_3O_4_NPs peak intensity, confirming the presence of Fe_3O_4 in the hybrid composite, in an indication that indeed no chemical interaction occurred between the polypyrrole

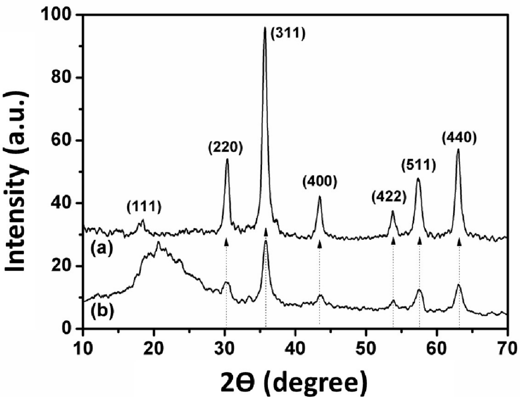

Figure 3. X-ray diffraction patterns of (a) Fe_3O_4_NPs and (b) Fe_3O_4_NPs/PPy.

and the magnetite. Thus, the crystalline structure of the iron oxide should be preserved. It could also be noted that a band at 2θ = 15.7-27.3° is observed, which corresponds to polypyrrole[29].

The infrared spectrum (FTIR) of the Fe_3O_4_NPs and Fe_3O_4_NPs/PPy composite is shown in Figure 4. For the Fe_3O_4_NPs/PPy composite, the presence of absorption bands at 1544, 1465, 1401, 1226 and 1078 cm^{-1} is observed, which is in agreement with data about polypyrrole reported in literature[30]. Such vibrational modes correspond to the stretching of C = C bonds (1544 cm^{-1}), CN (1226 cm^{-1}) and the connections[30] of the pyrrole rings (1465, 1401 and 1078 cm^{-1}). The infrared spectrum shows bands of Fe_3O_4_NPs at 638 and 584 cm^{-1}, which are characteristic of Fe-O bond vibrations[31]. These bands indicate the presence of magnetite in the nanocomposite.

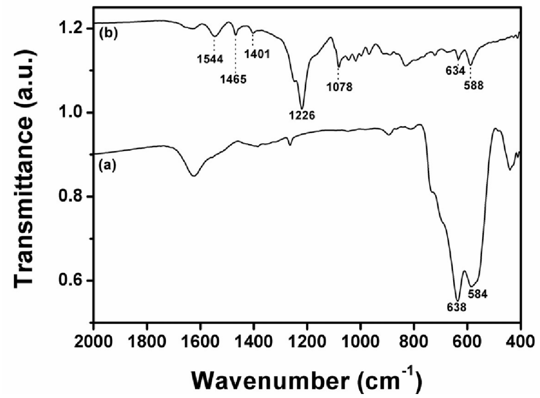

Figure 4. FTIR spectrum of (a) Fe_3O_4_NPs and (b) Fe_3O_4_NPs/PPy.

The anticorrosive performance of the Fe_3O_4_NPs/PPy in epoxy coatings on the SAE 1010 carbon steel plate was investigated by EIS measurements for two immersion times in a 3 wt% NaCl solution. Results shown in Figure 5 characterize the complete variation in the real and imaginary parts of impedance for all of the samples (Figures 5a and 5b), the dependence of the modulus of impedance and the phase with the frequency and the nature of the coating (Figures 5c and 5d), and the Nyquist plot with data fitted from the equivalent circuit (shown in the inset of Figure 5e) in which is possible to identify the bulk resistance (R_3), the charge transfer resistance (R_2) and a constant phase element (CPE) that fits the capacitive effects at interfaces and corresponding

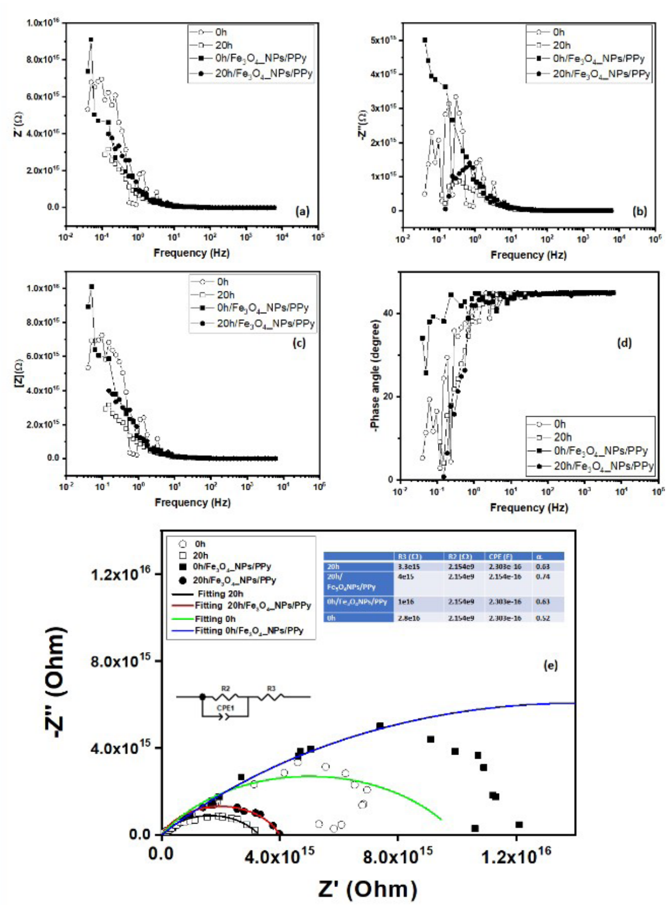

	R3 (Ω)	R2 (Ω)	CPE (F)	α
20h	3.3e15	2.154e9	2.303e-16	0.63
20h/ Fe_3O_4NPs/PPy	4e15	2.154e9	2.154e-16	0.74
0h/Fe_3O_4NPs/PPy	1e16	2.154e9	2.303e-16	0.63
0h	2.8e16	2.154e9	2.303e-16	0.52

Figure 5. Comparison of the electrical response of samples prepared by the coating of carbon steel plate coated with pure epoxy and with epoxy and Fe_3O_4_NPs/PPy 0.2% w/w after 0h and 20 h of immersion in saline solution in terms of the (a) real part of the impedance and (b) imaginary parts of the impedance versus frequency, (c) modulus of the impedance and (d) phase angle versus frequency. Nyquist diagrams for samples and the corresponding equivalent circuits with the fitting from solid lines with Table of data in the inset (e).

parameter (α) that is adjusted from 0 to 1 to reproduce the depressed behavior in a semicircle at Nyquist plot (an ideal capacitor is observed at α=1).

From the results shown in Figure 5a for the real part of impedance, it is possible to observe the general trend of reduction in the value with the frequency (a general behavior) that is also observed in the modulus of the impedance (see Figure 5c). The most important aspect to be considered from these results is a general reduction in the value of impedance for samples immersed in saline solution for 20 h, as a consequence of the corrosive process that results in the permeation of the saline solution in chains opened in the insulating coating (extremely high impedance). As a consequence, the reduction in the impedance can be explored as a direct parameter to measure the corrosion in the structure. In qualitative terms, it is possible to observe a stronger reduction for samples prepared in the absence of nanocomposite than in the presence of an additive, an indication that the effects of improvement in the anticorrosive activity can be attributed to the coating[32]. A more quantitative evaluation is shown by fitting parameters from an equivalent circuit. As can be seen from the inset of Figure 5e, the values for charge transfer follow the order: sample 0h>sample 0h/Fe_3O_4NPs/PPy> sample 20h/Fe_3O_4NPs/PPy> 20h. The higher values for samples previously to immersion in saline solution confirm the high values for charge transfer resistance of samples, while the stronger variation in the value after 20h of contact with a corrosive medium confirms that progressive corrosion in samples prepared in the absence of nanocomposite follows faster kinetics.

Recently, Pasha et al.[33] studied the use of organic composite coating consisting of epoxy (EP) reinforced with toluene sulphonic acid doped PPy embedded with manganese iron oxide ($MnFe_2O_2$) as a corrosion inhibitor for copper substrates. They investigated the variation of corrosion resistance with the time of immersion and the EIS measurements were conducted on all the samples upon exposure to 1 M HCl solution for 60 h. The authors concluded that the improved corrosion resistance can be attributed to the formation of the passive layer due to the presence of PPy and dispersed $MnFe_2O_2$ nanoparticles in the PPy matrix also behave as excellent physical barriers against the corrosive media.

In addition, Goswami et al.[34] worked on the synthesis of different structural forms of polyaniline (PANI) and their nanocomposites with graphene as functional fillers to epoxy coating for minimizing mild steel corrosion. Immersion studies were performed during 24 h to evaluate the influence of exposure time by EIS and to reveal the corrosion inhibition performance in 3.5 wt% NaCl electrolyte. Results highlighted that the conductive nature of the CP is believed to participate in the electron transfer mechanism to inhibit corrosion and the graphene skeleton in the graphene/PANI composite significantly improved the anticorrosive properties of corresponding PANI with multifold enhancement in total impedance.

These tests demonstrate that, as expected, the addition of Fe_3O_4_NPs/PPy increased the anticorrosive protection of epoxy coatings. This offers promising possibilities for the development of Fe_3O_4_NPs/PPy additives for anticorrosive paints.

4. Conclusions

In the present work, it is reported the synthesis of both Fe_3O_4_NPs obtained by co-precipitation and Fe_3O_4_NPs/PPy nanocomposites obtained by polymerization of pyrrole in the presence of SDS and Fe_3O_4_NPs. DLS measurements revealed that the Fe_3O_4_NPs and Fe_3O_4_NPs/PPy obtained have average diameters of (19.7 ± 9.6) nm and (63.5 ± 27.7) nm, respectively. TEM images confirmed that Fe_3O_4_NPs crystallize with a typical size of 10 - 30 nm and that Fe_3O_4_NPs/PPy nanocomposites were smaller than 100 nm, consisting of magnetite cores coated with polypyrrole. Finally, EIS measurements show that the addition of the Fe_3O_4_NPs/PPy nanocomposites to the epoxy paint allows greater anticorrosive efficiency in comparison to pure epoxy paints without any corrosion inhibitor. This behavior might be further exploited for the development of innovative hybrid nano pigments for corrosion protection. In addition, the study of other concentrations of Fe_3O_4_NPs/PPy and several immersion temperatures could be a great path in further studies to investigate the influence of the nanoparticles concentration on the efficiency of the coating.

5. Acknowledgments

The authors acknowledge the financial support from the Brazilian agencies Coordenação de Aperfeiçoamento de Pessoal de Nível Superior - Brasil (CAPES) - Finance Code 001 and Fundação de Amparo à Ciência e Tecnologia de Pernambuco – FACEPE (Grants APQ- 0916-3.03/14).

6. References

1. Roberge PR. Handbook of corrosion engineering. 2nd ed. New York: McGraw-Hill; 2012.
2. Veedu KK, Mohanb S, Somappa SB, Gopalan NK. Eco-friendly anticorrosive epoxy coating from Ixora leaf extract: a promising solution for steel protection in marine environment. J Clean Prod. 2022;340:130750.
3. DeBerry DW. Modification of the electrochemical and corrosion behavior of stainless steels with an electroactive coating. J Electrochem Soc. 1985;132(5):1022-6.
4. MacDiarmid AG, Ahmad N. Inhibition of corrosion of steels by conducting polymers. Abstracts of Papers of the American Chemical Society. 1987;193:58-9.
5. Li C, Zhang C, He Y, Li H, Zhao Y, Li Z, et al. Benzotriazole corrosion inhibitor loaded nanocontainer based on g-C3N4 and hollow polyaniline spheres towards enhancing anticorrosion performance of waterborne epoxy coatings. Prog Org Coat. 2023;174:107276.
6. Goswami RN, Mourya P, Behera B, Om P, Khatri OP, Ray A. Graphene-polyaniline nanocomposite based coatings: role of convertible forms of polyaniline to mitigate steel corrosion. Appl Surf Sci. 2022;599:153939.
7. Ohtsuka T. Corrosion protection of steels by conducting polymer coating. Int J Corros. 2012;2012:915090. http://dx.doi.org/110.1155/2012/915090.
8. Najmi P, Keshmiri N, Ramezanzadeh M, Ramezanzadeh B. Synthesis and application of Zn-doped polyaniline modified multi-walled carbon nanotubes as stimuli-responsive nanocarrier in the epoxy matrix for achieving excellent barrier-self-healing corrosion protection potency. Chem Eng J. 2021;412:128637.
9. Li X, Liu X, Liu H, Liu X, He R, Meng S. Structure, morphology and anti-corrosion performance of polyaniline modified

molybdenum sulfide/epoxy composite coating. Colloids Surf A Physicochem Eng Asp. 2022;639:128345.

10. Dalmoro V, Cedron S, Azambuja DS, Castagno KRL. Polypyrrole film doped with corrosion-inhibitors electropolymerized on AA 1100. Mater Res. 2019;22(Suppl. 1):e20180919.
11. Armelin A, Pla R, Liesa F, Ramis X, Iribarren JI, Alemán C. Corrosion protection with polyaniline and polypyrrole as anticorrosive additives for epoxy paint. Corros Sci. 2008;50(3):721-8. http://dx.doi.org/110.1016/j.corsci.2007.10.006.
12. Tang H, Liang Y, Liu C, Hu Z, Deng Y, Guo H, et al. A solution-processed n-type conducting polymer with ultrahigh conductivity. Nature. 2022;611(7935):271-7.
13. Jadhav, N.; Kasisomayajula S.; Gelling, V.J. Polypyrrole/metal oxides-based composites/nanocomposites for corrosion protection. Front Mater. 2020;7:95. https://doi.org/10.3389/fmats.2020.00095
14. Valença DP, Alves KGB, Melo C, Bouchonneau N. Study of the efficiency of polypyrrole/ZnO nanocomposites as additives in anticorrosion coatings. Mater Res. 2015;18(Suppl 2):273-8. http://dx.doi.org/110.1590/1516-1439.371614.
15. Hosseini MG, Bagheri R, Najjar R. Electropolymerization of polypyrrole and polypyrrole ZnO nanocomposites on mild steel and its corrosion protection performance. J Appl Polym Sci. 2011;121:3159-66.
16. Sharma S, Sudhakara P, Omran AAB, Singh J, Ilyas RA. Recent trends and developments in conducting polymer nanocomposites for multifunctional applications. Polymers (Basel). 2021;13:2898. http://dx.doi.org/110.3390/polym13172898.
17. Munhoza MGC, Rodrigues-Siquelib AC, Fonseca BCS, Marcuzo JS, Matsushimad JT, Lenz e Silva GFB, et al. Amaral-Labat. electrochemical properties of iron oxide decorated activated carbon cloth as a binder-free flexible electrode. Mater Res. 2022;25:e20220142.
18. Tie-Hong S, Yan-Jiao G, Su-Yan P, Rui-Hua H, Han-Bo L. Study of Fe_3O_4/PS system in degrading BPA in aqueous solution. J Braz Chem Soc. 2021;32(12):2264-71.
19. Taufiq A, Iswatin AD, Saputro RE, Yogihati CI, Hidaya N, Diantoro M. Sunaryono, munasir, fabrication of new Fe_3O_4/PVA/$(C_6H_7O_6Na)_n$ nanohybrid ferrogels for antibacterial applications. Mater Res. 2021;24(2):e20200232.
20. Garcia B, Lamzoudi A, Pillier F, Nguyen H, Le T, Deslouis C. Oxide/polypyrrole composite films for corrosion protection of iron. J Electrochem Soc. 2002;149:B560-6.
21. Alves KGB, Andrade CAS, Campello SL, de Souza RE, de Melo CP. Magnetite/polypyrrole hybrid nanocomposites as a promising magnetic resonance imaging contrast material. J Appl Polym Sci. 2013;128(5):3170-6.
22. Delimi A, Ferkous H, Alam M, Djellali S, Sedik A, Abdesalem K, et al. Corrosion protection performance of silicon-based coatings on carbon steel in NaCl solution: a theoretical and experimental assessment of the effect of plasma-enhanced chemical vapor deposition pretreatment. RSC Advances. 2022;12:15601-12. http://dx.doi.org/110.1039/D1RA08848C.
23. Kameneva A, Kichigin V, Bublik N. Effect of structure, phase, and elemental composition of AlN, CrAlN, and ZrAlN coatings on their electrochemical behavior in 3% NaCl solution. Materials and Corrosion. 2022;73(8):1308-17. https://doi.org/10.1002/maco.202213073
24. Shi X, Nguyen TA, Suo Z, Liu Y, Avci R. Effect of nanoparticles on the anticorrosion and mechanical properties of epoxy coating. Surf Coat Tech. 2009;204(3):237-45. http://dx.doi.org/110.1016/j.surfcoat.2009.06.048.
25. Hermas AA. Protection of type 430 stainless steel against pitting corrosion by ladder conductive polymer. Prog Org Coat. 2008;61(1):95-102. http://dx.doi.org/110.1016/j.porgcoat.2007.09.005.
26. Le HNT, Garcia B, Deslouis C, Le Xuan Q. Corrosion protection and conducting polymers: polypyrrole films on iron. Electrochim Acta. 2001;46(26-27):4259-72. http://dx.doi.org/110.1016/S0013-4686(01)00699-5.
27. Ahmed MA, El-Dek SI, Abd Elazim A. Fascinating properties of multifunctional nanocomposites manganite/magnetite. Superlattices Microstruct. 2014;74:34-51.
28. Liu HL, Wu J, Min JH, Kim YK. One-pot synthesis and characterization of bifunctional Au-Fe_3O_4 hybrid core-shell nanoparticles. J Alloys Compd. 2012;537:60-4.
29. Chougule MA, Sen S, Patil VB. Facile and efficient route for preparation of polypyrrole-ZnO nanocomposites: Microstructural, optical, and charge transport properties. J Appl Polym Sci. 2012;125:E541-7.
30. Melo EF, Alves KGB, Junior SA, Melo CP. Synthesis of fluorescent PVA/polypyrrole-ZnO nanofibers. J Mater Sci. 2013;48(10):3652-8.
31. Habibi N. Preparation of biocompatible magnetite-carboxymethyl cellulose nanocomposite: characterization of nanocomposite by FTIR, XRD, FESEM and TEM. Spectrochim Acta A Mol Biomol Spectrosc. 2014;131:55-58.
32. Gonzalez MB, Saidman SB. Corrosion protection properties of polypyrrole electropolymerized onto steel in the presence of salicylate. Prog Org Coat. 2012;75(3):178-83.
33. Pasha A, Khasim S, Darwish AAA, Hamdalla TA, Al-Ghamdi SA. High performance organic coatings of polypyrrole embedded with manganese iron oxide nanoparticles for corrosion protection of conductive copper surface. J Inorg Organomet Polym Mater. 2022;32(2):499-512.
34. Goswami RN, Mourya P, Behera B, Khatri OP, Ray A. Graphene-polyaniline nanocomposite based coatings: role of convertible forms of polyaniline to mitigate steel corrosion. Appl Surf Sci. 2022;599:153939.